Cancer Cell
Article

Germline *Brca2* Heterozygosity Promotes *Kras*^{G12D} -Driven Carcinogenesis in a Murine Model of Familial Pancreatic Cancer

Ferdinandos Skoulidis,[1] Liam D. Cassidy,[1] Venkat Pisupati,[1] Jon G. Jonasson,[2] Hordur Bjarnason,[3] Jorunn E. Eyfjord,[3] Florian A. Karreth,[4] Michael Lim,[1] Lorraine M. Barber,[1] Susan A. Clatworthy,[1] Susan E. Davies,[5] Kenneth P. Olive,[6] David A. Tuveson,[4] and Ashok R. Venkitaraman[1,*]

[1]Department of Oncology and the Medical Research Council Cancer Cell Unit, University of Cambridge, Hills Road, Cambridge CB2 0XZ, UK
[2]Department of Pathology, Faculty of Medicine, Landspitalinn–University Hospital, University of Iceland and The Icelandic Cancer Registry, Reykjavik, Iceland
[3]Cancer Research Laboratory, Faculty of Medicine, University of Iceland, Vatnsmyrarvegi 16, 101 Reykjavik, Iceland
[4]Li Ka Shing Centre, Cambridge Research Institute, Cancer Research UK, Robinson Way, Cambridge CB2 0RE, UK
[5]Addenbrooke's Hospital, Cambridge CB2 2QQ, UK
[6]Herbert Irving Comprehensive Cancer Center and Department of Medicine and Pathology, Columbia University, New York, NY 10032, USA
*Correspondence: arv22@cam.ac.uk
DOI 10.1016/j.ccr.2010.10.015

SUMMARY

Inherited heterozygous *BRCA2* mutations predispose carriers to tissue-specific cancers, but somatic deletion of the wild-type allele is considered essential for carcinogenesis. We find in a murine model of familial pancreatic cancer that germline heterozygosity for a pathogenic *Brca2* truncation suffices to promote pancreatic ductal adenocarcinomas (PDACs) driven by *Kras*^{G12D}, irrespective of *Trp53* status. Unexpectedly, tumor cells retain a functional *Brca2* allele. Correspondingly, three out of four PDACs from patients inheriting *BRCA2*^{999del5} did not exhibit loss-of-heterozygosity (LOH). Three tumors from these patients displaying LOH were acinar carcinomas, which also developed only in mice with biallelic *Brca2* inactivation. We suggest a revised model for tumor suppression by BRCA2 with implications for the therapeutic strategy targeting *BRCA2* mutant cancer cells.

INTRODUCTION

The *BRCA2* tumor suppressor gene encodes a nuclear protein of 3418 residues (3328 in the mouse) with a pivotal role in the maintenance of chromosome stability via homology-directed DNA repair (reviewed in Venkitaraman, 2009). Concordant with the "two-hit" paradigm for tumor suppression (Knudson, 1971), somatic deletion of the wild-type *BRCA2* allele has been reported to occur consistently in breast or ovarian cancer cells from mutation carriers (Collins et al., 1995; Gudmundsson et al., 1995) and is therefore regarded as an essential event in carcinogenesis. This principle underlies the clinical use of PARP1 inhibitors, because these drugs selectively kill *BRCA2*-null but not *BRCA2*-heterozygous cells in vitro (Audeh et al., 2010; Bryant et al., 2005; Farmer et al., 2005; Fong et al., 2009; 2010; Tutt et al., 2010).

Germline carriers of deleterious *BRCA2* mutations that commonly truncate the encoded protein exhibit an increased lifetime risk of developing pancreatic ductal adenocarcinoma (PDAC), in addition to their well-known predisposition to cancers of the breast and ovary (Breast Cancer Linkage Consortium 1999). Within high-risk pancreatic cancer kindreds, inherited mutations in *BRCA2* may represent the most frequently encountered germline genetic alteration (Couch et al., 2007; Hahn et al.,

Significance

Our findings raise the possibility that, contrary to current understanding, *BRCA2* LOH may not be essential for pancreatic ductal carcinogenesis in mutation carriers, and a significant proportion of tumors in these patients may retain a functional *BRCA2* allele. If so, therapeutic agents that selectively kill BRCA2-deficient cancer cells, such as poly-ADP-ribose polymerase (PARP1) inhibitors, should preferably be used after tumor LOH has been confirmed. Our findings also suggest that biallelic *BRCA2* inactivation promotes a distinct tumor type, acinar carcinoma of the pancreas, that might therefore be more vulnerable to targeted therapies. Our work revises the conceptual understanding of tissue-specific carcinogenesis associated with *BRCA2* mutations and may help to improve the design of clinical trials using targeted agents.

2003). Some apparently sporadic pancreatic cancers are also found to harbor germline *BRCA2* mutations, because a positive family history is frequently lacking (Goggins et al., 1996). More recently, *PALB2*, which encodes a BRCA2-interacting protein also essential for homology-directed DNA repair, has emerged as a pancreatic cancer-susceptibility allele (Jones et al., 2009). Although these findings collectively highlight its potential importance, the role played by *BRCA2* inactivation in pancreatic carcinogenesis remains unclear.

Several of the most frequent genetic events underlying the initiation and progression of human pancreatic cancer have been identified (Hezel et al., 2006; Maitra and Hruban, 2008). Notably, activating mutations in the *KRAS* proto-oncogene occur in > 90% of PDAC (Caldas and Kern, 1995) and are considered as a key driver for pancreatic carcinogenesis, whereas mutations inactivating the *TP53* gene occur in 50%–75% of patients (Redston et al., 1994). A cooperative effect between *Kras* activation and *Trp53* inactivation in promoting pancreatic carcinogenesis has been demonstrated in murine models (Hingorani et al., 2005). Here, we have exploited these findings to develop a mouse model for familial pancreatic cancer associated with *BRCA2* inactivation.

RESULTS

We utilized the well-validated KPC murine model of PDAC (Hingorani et al., 2003, 2005; Olive et al., 2004, 2009), in which Cre-*lox*P recombination in *Pdx1*-CRE (C) expressing pancreatic progenitors directs the tissue-specific activation of endogenous oncogenic $Kras^{G12D}$ (K), with or without concurrent expression of the $Trp53^{R270H}$ (P) dominant-negative contact mutant. We introduced into this setting two distinct mutant alleles of *Brca2* (B). The first encodes the germline-truncating allele $Brca2^{Tr}$ (abbreviated Tr), which terminates the encoded protein at amino acid (aa) 1492, and mimics known pathogenic mutations in human *BRCA2* associated with pancreatic cancer (Friedman et al., 1998; Hahn et al., 2003). This allele emulates *BRCA2* heterozygosity in all somatic tissues, characteristic of human mutation carriers. The second allele is a conditional *Brca2* deletion (abbreviated F11), in which *lox*P sites flank the evolutionarily conserved *Brca2* exon 11 that encodes binding sites for the Rad51 recombinase (Wong et al., 1997) and is critical for Brca2's function in DNA repair (Chen et al., 1998). This enables Cre-mediated exon 11 deletion (abbreviated Δ11) in specific tissues, emulating the loss-of-heterozygosity (LOH) observed in human cancers by gross genomic rearrangements in *BRCA2* (Jonkers et al., 2001). Experimental mice were maintained on a mixed C57BL/6; 129; FVB/N genetic background, and all experiments were performed using littermate controls in order to ensure that comparisons were between mice on the same genetic background. Figure 1A schematically represents the alleles used to engineer KPCB and KCB strains (i.e., with or without $Trp53^{R270H}$), harboring the different *Brca2* genotypes.

Cre expression in the *Pdx1*-defined pancreatic anlagen led to efficient recombination of all conditional alleles. This was verified by allele-specific polymerase chain reactions (PCRs) for the $Kras^{1\text{-}loxP}$, $Trp53^{1\text{-}loxP}$, $Brca2^{F11}$ and $Brca2^{\Delta 11}$ alleles in DNA extracted from microdissected cancerous ducts and early passage PDAC cell lines from $KPCB^{Tr/\Delta 11}$ mice (Figure 1B). Consistent with previous observations, loss of the wild-type *Trp53* allele was a universal event in tumors expressing mutant $Trp53^{R270H}$.

As expected, neither heterozygous nor homozygous *Brca2* inactivation in the murine pancreas was sufficient for pancreatic carcinogenesis without the concurrent expression of $Kras^{G12D}$. This is evident irrespective of Trp53 status, even after prolonged follow up (see Figure S1 available online), suggesting that Kras activation is necessary to initiate pancreatic carcinogenesis in this model.

Homozygous *Brca2* inactivation in the $KPCB^{Tr/\Delta 11}$ strain caused PDAC at a high penetrance, with a rapid and predictable clinical decline (median PDAC-free survival 84 days, range 48–110 days) compared with the KPCB cohort carrying wild-type *Brca2* (median PDAC-free survival 168 days, range 60–254 days) (Figure 1C). Remarkably, however, germline heterozygosity for the truncating allele $Brca2^{Tr}$ in the $KPCB^{Tr/WT}$ strain also curtailed PDAC-free survival compared with KPCB animals who had wild-type *Brca2* (median PDAC-free survival 143 days, range 91-191 days; p = 0.0013, log-rank test) (Figure 1C). Germline heterozygosity for $Brca2^{Tr}$ was sufficient to promote carcinogenesis, even in $KCB^{Tr/WT}$ mice with wild-type *Trp53* and mutant $Kras^{G12D}$, a background in which frank pancreatic cancer is reported to develop less readily (Hingorani et al., 2003). Thus, there is a statistically significant reduction in the PDAC-free survival of $KCB^{Tr/WT}$ mice in comparison with KCB controls with wild-type *Brca2* (p = 0.0149, log rank test) (Figure 1D). A similar cancer-promoting effect for germline *Brca2* heterozygosity has not hitherto been reported in any constitutive or conditional murine model of *Brca2* deficiency.

Interestingly, in $KCB^{Tr/\Delta 11}$ mice with wild-type *Trp53*, *Pdx1*-Cre mediated loss of the second *Brca2* allele in the pancreas frequently caused pancreatic insufficiency, necessitating the sacrifice of 25% of the animals in this cohort (8/32) at a median age of 63.5 days (range 51–121). We observed a spectrum of histological anomalies, from isolated paucity of the islets of Langerhans to complete fibro-inflammatory or cystic degeneration of both the endocrine and exocrine pancreas (Figure 2A). This suggests that many *Brca2*-deficient cells expressing $Kras^{G12D}$ in these compartments cannot survive when Trp53-dependent cell cycle checkpoints responsive to DNA breakage are intact, in agreement with prior observations in other experimental systems (Ludwig et al., 1997). Consistent with this inference, pancreata from 6 day old $KCB^{Tr/\Delta 11}$ neonatal mice exhibit both a marked increase in the abundance of apoptotic cells as well as in staining for the phosphorylated form of the variant histone H2AX, a marker for double-strand DNA breaks, when compared with $KCB^{WT/WT}$, $KCB^{Tr/WT}$, $CB^{WT/WT}$, or $CB^{Tr/WT}$ littermate controls (Figure S2). Interestingly, animals in this cohort that did not succumb to pancreatic insufficiency later developed PDAC with a moderate latency and incomplete penetrance, but nevertheless exhibited significantly shortened PDAC-free survival compared with KCB controls with wild-type *Brca2* (p = 0.0114, log rank test) (Figure 1D).

Pancreatic tumors originating in the setting of *Brca2* heterozygosity (with or without mutant *Trp53*) displayed histological features remarkably similar to human pancreatic cancers. Most had a morphology closely resembling human PDAC, with abundant desmoplastic stroma surrounding the cancerous glands

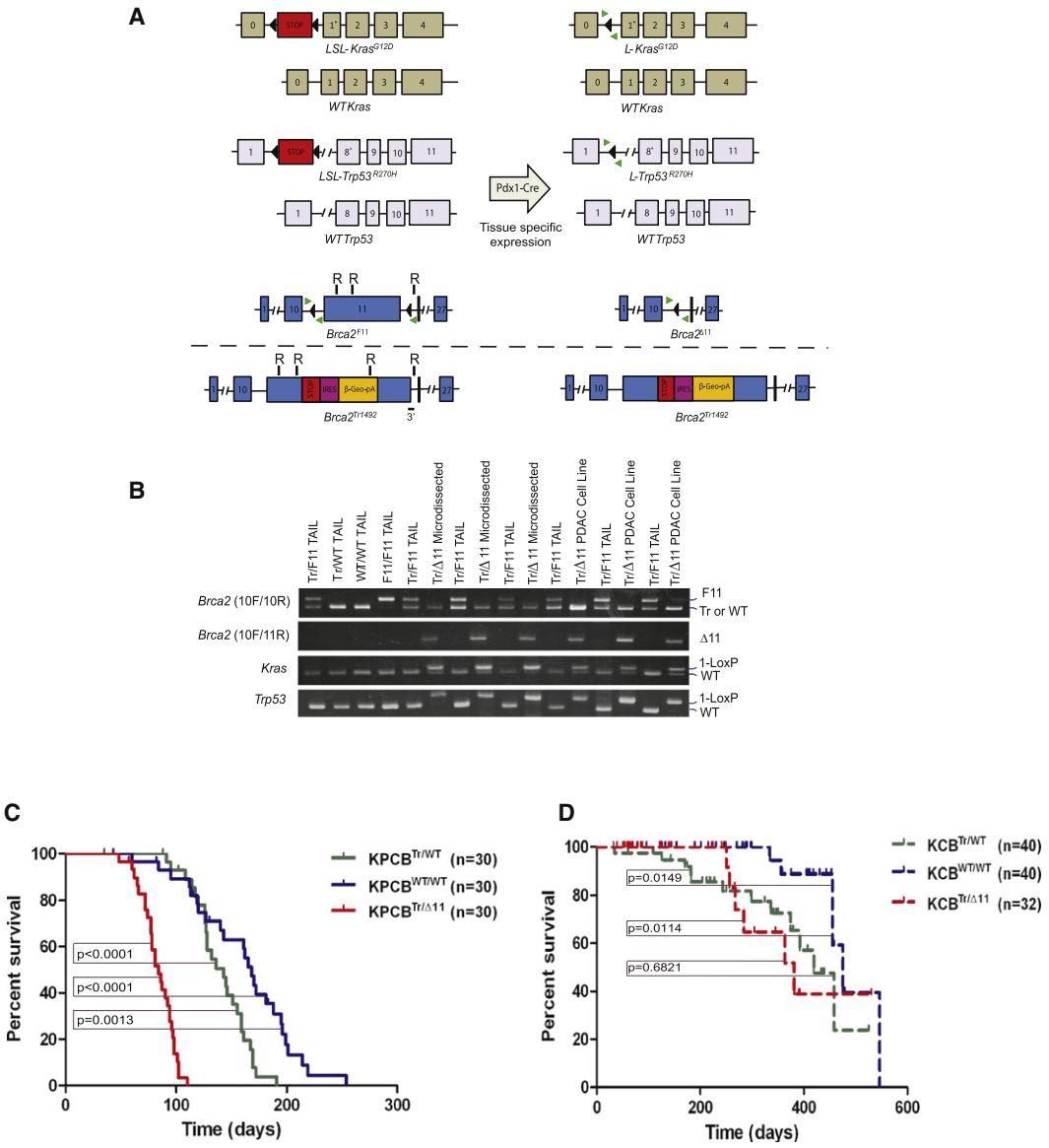

Figure 1. *Brca2* Mutations Promote Pancreatic Carcinogenesis Driven by Oncogenic *Kras* ^{G12D} with or without Concurrent Mutant *Trp53*^{R270H} Expression

(A) Schematic representation of the targeted alleles before and after Cre-mediated recombination. The *Brca2*^{Tr} allele (bottom) is expressed in all somatic tissues. (B) Recombination of the conditional alleles in cell lines and microdissected cancerous ducts from KPCB$^{Tr/\Delta 11}$ mice revealed by semiquantitative PCR. Tail DNA is used as a control. PCR primer pairs are indicated by red arrows in (A); their sequences are in Supplemental Experimental Procedures.

(C and D) Kaplan-Meier estimates of PDAC-free survival in aging KPCB (C) and KCB (D) cohorts. The *Brca2* genotype is indicated. The log rank test was used for all the indicated statistical comparisons. The only pair-wise comparison that is not statistically significant is marked p = 0.6821.See also Figure S1.

(Figures 2B and 2C). These tumors evolved along the pancreatic intraepithelial neoplasia (PanIN) cascade (Figures 3A–3F), well characterized in human pancreatic cancers (Hruban et al., 2001), and exhibited characteristic patterns of invasive growth and metastatic behavior (Figures 3G–3L). Less common histological variants of human pancreatic cancer, predominantly undifferentiated carcinoma with sarcomatoid and anaplastic features, were also represented (Figures 2D and 2E). Prominent intra-tumoral heterogeneity was frequently present, with distinct histological appearances often evident in adjacent regions of the same tumor. Interestingly, the KPCB$^{Tr/\Delta 11}$ cohort, which carries biallelic *Brca2* mutations, uniquely developed an acinar-cell carcinoma component in ~18% of assessable cases (5/28), not observed in the other cohorts with *Brca2* heterozygosity (Figures 2F–2H). Furthermore, one tumor within this cohort (1/28) displayed a small component with prominent immunohistochemical positivity for chromogranin A, characteristic of endocrine neoplasms (Figure 3J; data not shown). Collectively, our observations suggest that *Brca2* inactivation promotes the evolution of oncogenic *Kras*-driven pancreatic malignancies

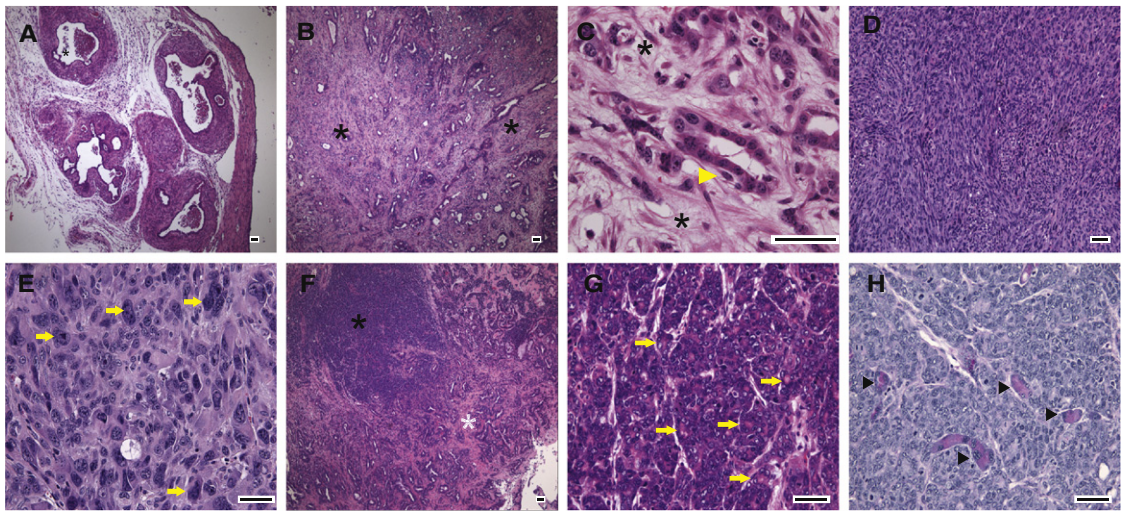

Figure 2. Representative Histological Appearances of Pancreatic Malignancies in KPCB and KCB Mice

(A) Intense fibro-inflammatory obliteration of the normal acinar structure with ductal cystic dilatation, replacing the pancreatic parenchyma in a 62 day old $KCB^{Tr/\Delta 11}$ mouse with clinical signs of pancreatic insufficiency.

(B) Classical "haphazard" growth pattern of a well-differentiated PDAC in a 4 month old $KPCB^{Tr/WT}$ mouse. Abundant desmoplastic stroma surrounds the cancerous ducts (*).

(C) High-magnification image of a moderately differentiated adenocarcinoma. The irregular glandular structures, composed of moderately pleomorphic cells (yellow arrowhead), are surrounded by desmoplastic stroma (*).

(D) A sarcomatoid tumor from the $KPCB^{Tr/\Delta 11}$ strain, with mildly pleomorphic spindle cells arranged in intervening fascicles.

(E) Anaplastic pancreatic cancer. Note the completely bizarre nuclei and the characteristic noncohesive growth pattern of malignant cells in this histological subtype (yellow arrow).

(F) Ductal-type adenocarcinoma (white asterisk) coexists with an acinar-cell carcinoma (*) within the same imaging field in a 3.5 month old $KPCB^{Tr/\Delta 11}$ mouse.

(G) Higher-power view of acinar-cell carcinoma from a second $KPCB^{Tr/\Delta 11}$ mouse showing malignant cells with granular eosinophilic apical cytoplasm (and frequently a single prominent nucleolus); several minute lumina, resembling normal acini (yellow arrow), are evident and intervening stroma is scarce.

(H) Foci of intracytoplasmic granular positivity with dPAS staining (arrowhead) within an acinar-cell carcinoma from a different $KPCB^{Tr/\Delta 11}$ mouse. Scale bar = 50 μm. See also Figure S2.

in mice that are strikingly similar to their human counterparts, providing a valuable resource for future studies. Table 1 summarizes the features and histological characteristics of PDAC arising in the different cohorts.

To validate our conclusion that *Brca2* heterozygosity suffices to promote carcinogenesis driven by oncogenic *Kras* in the pancreas, we gathered multiple independent lines of evidence to confirm that the remaining wild-type *Brca2* allele had been retained in tumors from $KPCB^{Tr/WT}$ and $KCB^{Tr/WT}$ animals. mRNA prepared from early passage cell lines derived from a panel of $KPCB^{Tr/WT}$ tumors was analyzed by quantitative reverse-transcription (RT)-PCR using a primer pair that amplifies a segment in the 3′ region of the *Brca2* mRNA (expected to be absent in transcripts from the $Brca2^{Tr}$ allele). The analysis showed that wild-type *Brca2* mRNA was expressed in these tumors at approximately half the levels observed in a control KPCB cell line carrying wild-type *Brca2*, consistent with transcription from a retained wild-type *Brca2* locus in the heterozygous tumors (Figure 4A). Western blotting for murine Brca2 protein using an N-terminal antibody confirmed expression of full-length Brca2 protein in heterozygous tumors (Figure 4B). Southern blots of genomic DNA extracted from snap-frozen whole pancreatic tumors arising in strains heterozygous for *Brca2* further demonstrated that the wild-type allele was retained in vivo (Figure 4C; Figure S3A), arguing against the possibility that tumors with *Brca2* deletion were present but failed to grow out in ex vivo cultures. Finally, two distinct assays confirmed that the retained *Brca2* allele could express a functional Brca2 protein. Accumulation of the RAD51 enzyme in nuclear foci induced by DNA damage requires functional BRCA2 (Yuan et al., 1999). Indeed, tumor-derived cell lines from $KPCB^{Tr/WT}$ mice heterozygous for *Brca2* robustly induce Rad51 nuclear foci when exposed to mitomycin C (MMC), a genotoxin known to engage Brca2-dependent DNA repair. In contrast, baseline and MMC-induced nuclear Rad51 foci were suppressed in tumor-derived cell lines from $KPCB^{Tr/\Delta 11}$ mice lacking both *Brca2* alleles (Figures 4D and 4E). Similarly, $KPCB^{Tr/WT}$ tumor cell lines with a retained *Brca2* allele were more resistant to MMC and the poly-ADP-ribose polymerase (PARP1) inhibitor Olaparib than similar cell lines from $KPCB^{Tr/\Delta 11}$ mice lacking both *Brca2* alleles (Figures 4F and 4G; Figures S3B–S3D), in agreement with previous reports (Farmer et al., 2005; van der Heijden et al., 2005). Collectively, our findings offer strong evidence that PDACs arising in strains heterozygous for *Brca2* mutations retain a functional second allele.

It is noteworthy that 24 of the 26 PDAC tumors arising in the $KPCB^{Tr/WT}$ animals included in our survival analysis demonstrated retention of the wild-type allele. DNA from one tumor was unavailable, whereas another tumor exhibited apparent LOH (Figure S3A). Their exclusion did not alter our statistical

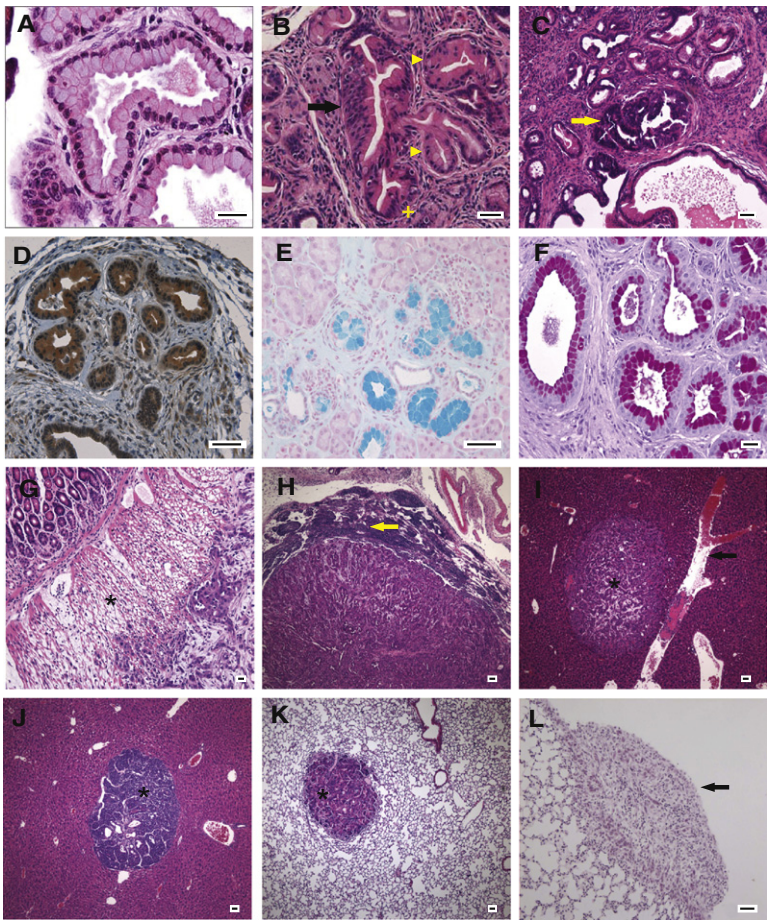

Figure 3. Murine Tumors Faithfully Recapitulate the Histological Progression and Metastatic Propensities of Human PDAC

(A) PanIN-1A in a 4 month old $KCB^{WT/WT}$ mouse.

(B) PanIN-2 (arrow) surrounded by PanIN-1A (yellow arrowhead) and PanIN-1B (yellow cross) in a 8.75 month old $KCB^{Tr/WT}$ mouse.

(C) PanIN-3 (yellow arrow) in a 6.25 month old $KPCB^{Tr/WT}$ mouse.

(D–F) Positive immunostaining for Cytokeratin-19 confirms the ductal phenotype of PanIN lesions that also stain positive with the Alcian blue (E) and dPAS (F) histochemical stains due to their high mucin content.

(G) Prominent duodenal invasion in a moderately-differentiated $KPCB^{Tr/WT}$ tumor (*).

(H) Involvement of a peripancreatic lymph node by a moderately/poorly differentiated pancreatic adenocarcinoma (yellow arrow).

(I and J) Liver metastases (*) from a poorly differentiated PDAC (I) and predominantly endocrine (J) neoplasm. Note the blood vessel in close anatomical proximity to the tubular metastasis (arrow).

(K and L) (K) Parenchymal lung metastasis (*) and (L) pleural metastasis (arrow). Scale bar = 50 μm.

conclusions from the survival analysis, ruling out the possibility that loss of the wild-type *Brca2* allele in a very small fraction of $KPCB^{Tr/WT}$ tumors might account for the observed differences.

A founder mutation in human *BRCA2* (999del5) has an allele frequency of ~0.6% in the general population of Iceland, but accounts for about 40% of familial breast and ovarian cancer cases in this population (Thorlacius et al., 1996, 1997). $BRCA2^{999\ del5}$ encodes an unstable protein that is undetectable in cells heterozygous for the allele (Mikaelsdottir et al., 2004). We traced seven known cases of pancreatic cancer (Table 2) arising in carriers of the 999del5 allele through the Icelandic Cancer Registry. Four of these tumors represent typical PDACs (Figures 5A–5D) whereas the remaining three were characterized as acinar cell carcinomas based on their morphology, immunohistochemical positivity for chymotrypsin and trypsin, and their lack of expression of ductal or endocrine markers (Figures 5E–5H; data not shown). DNA samples extracted from microdissected cancerous ducts were analyzed for allelic ratios of the wild-type and mutant *BRCA2* alleles using allele-specific PCR, which strongly correlates with changes in copy number over the entire *BRCA2* locus by array CGH (Figure S4). Remarkably, three out of the four tumor samples with typical ductal histology (75%) did not exhibit LOH at the mutation site. On the contrary, all three acinar carcinomas demonstrated LOH for $BRCA2^{999\ del5}$ (Figure 5I and Table 2; Figure S4).

Table 1. Clinical Features and Histological Characteristics of Pancreatic Tumors Arising in Different Mouse Cohorts

			PDAC-free survival		Histology			
Genotype	n	PDAC	Median	Range	Tubular	Sarcomatoid	Anaplastic	Acinar
$KPCB^{WT/WT}$	30	24	168	60–254	92 (92)	8 (21)	0 (4)	0 (0)
$KPCB^{Tr/WT}$	30	26	143	91–191	96 (100)	4 (15)	0 (4)	0 (0)
$KPCB^{Tr/\Delta 11}$	30	29	84	48–110	82 (100)	18 (54)	0 (7)	0 (18)
$KCB^{WT/WT}$	40	6	N/A	N/A	83 (100)	17 (50)	0 (0)	0 (0)
$KCB^{Tr/WT}$	40	12	N/A	N/A	100 (100)	0 (17)	0 (0)	0 (0)
$KCB^{Tr/\Delta 11}$	32	6	N/A	N/A	83 (100)	17 (33)	0 (17)	0 (0)

In assessing the contributions of different histological appearances, the reported numbers refer to the percentage of tumors within each cohort where the particular histology predominates (occupies more than 50% of the total tumor area), whereas numbers in parentheses represent the percentage of tumors with any component of the indicated histology present. Percentage calculations are based on the numbers of histologically assessable tumors within each cohort.

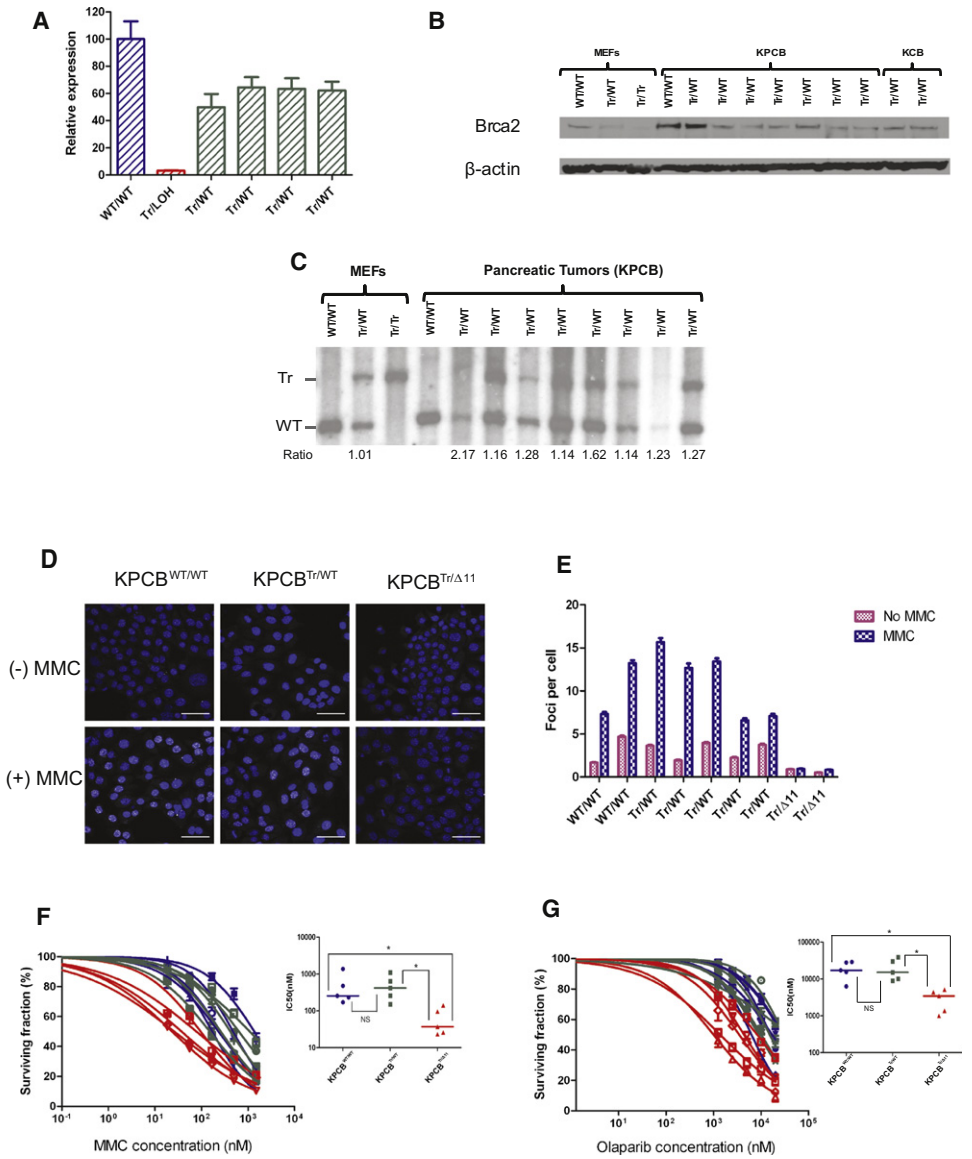

Figure 4. Retention of a Functional *Brca2* Allele in PDAC Cell Lines and Tumors from *Brca2* Heterozygote Mice

(A) Quantitative RT-PCR was performed on mRNA from KPCB PDAC lines of the specified genotypes, using primers recognizing the 3′ end of murine *Brca2* (*Brca2* 22 Forward, *Brca2* 24 Reverse). "Tr/LOH" refers to a KCB$^{Tr/\Delta 11}$ PDAC line used as control (which has lost *Brca2* genomic sequences 5′ to the loxP site within intron 10). The graph shows Ct values normalized to the Ct values of *Gapdh* as a percent change compared with a PDAC line homozygous for wild-type *Brca2*. Error bars represent standard deviation (SD) from the mean of triplicate reactions.

(B) Western blot of murine Brca2 protein using an antibody against the N-terminal region in whole cell lysates from KPCB$^{Tr/WT}$ and KCB$^{Tr/WT}$ lines. β-actin serves as a loading control.

(C) Southern blot of EcoRI-digested tumor DNA using a 3′ probe, external to the IRES-βGeo-pA cassette. Densitometry was used to quantify the ratio of the intensity of the lower (3.1kb) band, representing the wild-type allele to that of the upper (3.9kb) band corresponding to mutant *Brca2*.

(D) Representative confocal images (x400) of Rad51 nuclear foci induced in KPCB lines by exposure to 100 ng/ml MMC for 24 hr. Scale bar = 50μm.

(E) A graph quantifying the experiments depicted in (D) using the Cellomics HCS Arrayscan VTI (ThermoFisher) shows the average number of nuclear Rad51 foci per cell ($n \geq 800$ cells in each sample). DAPI-stained nuclei are shown in blue, whereas Rad51 foci are represented in white. Error bars represent the standard error of the mean (SEM) from 20 imaging fields per sample.

(F and G) Viability curves of representative KPCB lines following exposure for 72 hr either to Mitomycin C (F) or the PARP1 inhibitor, Olaparib (G).Error bars represent SD from the mean value from quintuplicate wells. Median IC_{50} values for MMC and Olaparib differed significantly across the three groups (KPCB carrying wild-type *Brca2*, KPCB$^{Tr/WT}$, and KPCB$^{Tr/\Delta 11}$) ($p = 0.0090$ and $p = 0.0092$, respectively; Kruskal-Wallis test). Dunn's post-test was used for individual comparisons between the three groups ($n = 5$ for each group). Asterisks denote statistical significance at $p < 0.05$. See also Figure S3.

Table 2. Clinical Features and *BRCA2*^{999del5} LOH Analysis in Seven Pancreatic Cancer Cases from Confirmed Carriers of this Icelandic Founder Mutation

Sample identifier	Sex	Age at diagnosis	LOH at *BRCA2*$^{999\ del5}$	Histology	Other pathologies
s1	M	70	Y	Acinar-cell carcinoma (head)	N/A
s7	F	59	Y	Acinar-cell carcinoma (head)	Lobular breast cancer (58)
s5	M	43	N	Adenocarcinoma (moderately differentiated)	N/A
s9	F	50	N	Adenocarcinoma (moderately differentiated)	Ductal breast cancer; myxopapillary ependymoma (48)
s10	F	78	Y	Adenocarcinoma (moderately differentiated)	N/A
s3	M	71	Y	Acinar-cell carcinoma	N/A
s8	M	67	N	Adenocarcinoma NOS (tail)	N/A

The number in brackets in the last column refers to age in years at diagnosis.

DISCUSSION

We suggest, on the basis of our findings, a revised model for carcinogenesis associated with BRCA2 deficiency in the pancreas (Figure 6), which incorporates several interesting features. We find that germline heterozygosity for *Brca2* mutations suffices to promote the development of *Kras*^{G12D}-driven pancreatic ductal adenocarcinomas, typically representing >90% of human pancreatic tumors, irrespective of the functional status of *Trp53*. Unexpectedly, these tumors retain

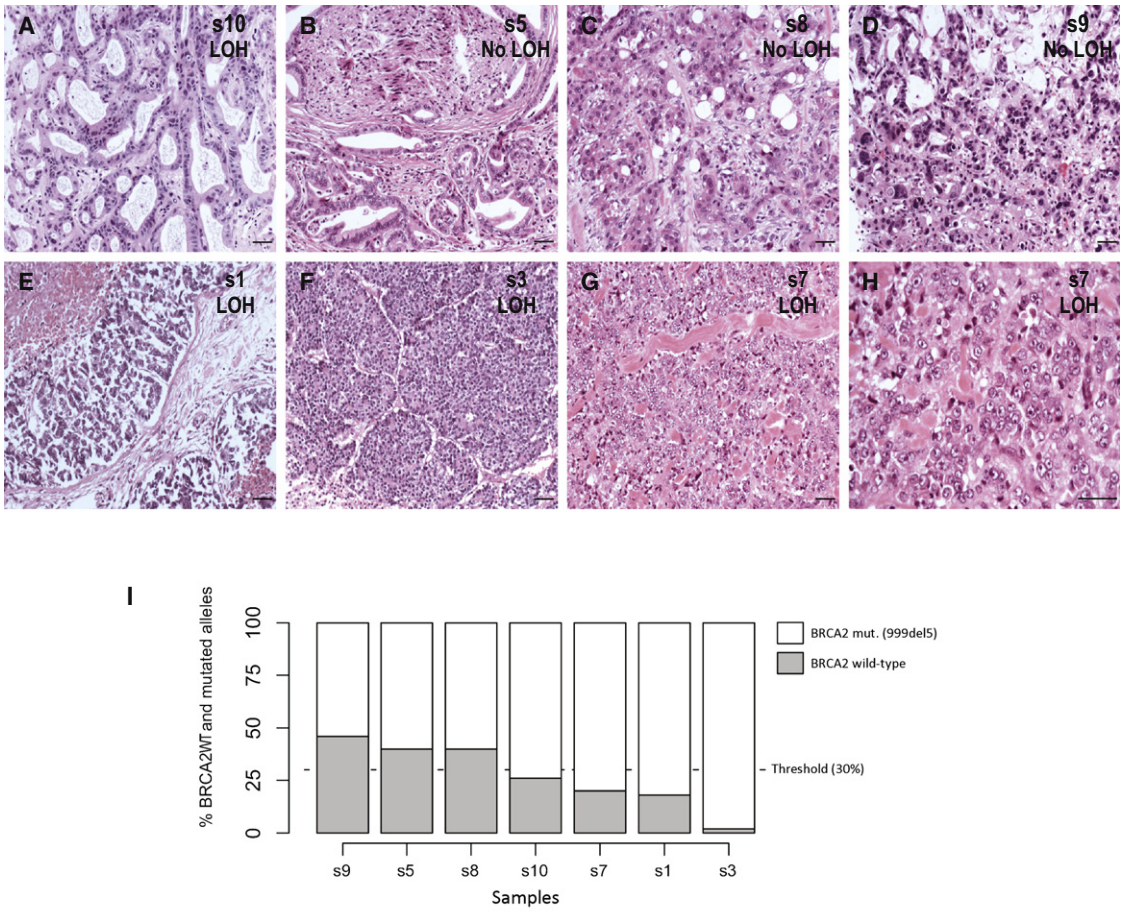

Figure 5. *BRCA2* Alleles in Pancreatic Cancers from Carriers of the 999del5 Mutation

(A–H) Histology of pancreatic neoplasms in confirmed carriers of the pathogenic *BRCA2*^{999del5} mutation.

(I) Allele-specific quantification of wild-type and mutant *BRCA2* alleles in seven human pancreatic tumor samples using quantitative RT-PCR. The proportion of *BRCA2* alleles, wild-type (gray) and mutated (white), is displayed for individual tumors. The threshold line for determining loss of the wild-type allele ($\leq$30%) is based on concordance with copy number changes measured by array CGH. See also Figure S4.

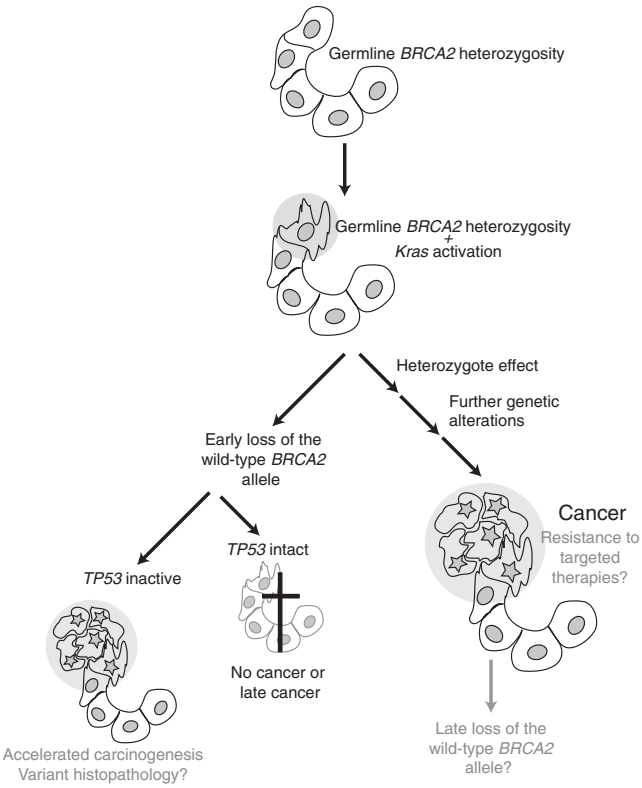

Figure 6. A Revised Model for Tumor Suppression by *BRCA2*

Our work models germline inheritance of the $Brca2^{Tr}$ allele in all somatic tissues (first hit, top), and $Kras^{G12D}$ activation in the pancreas (second hit), combined either with early LOH of the second *Brca2* allele (third hit, left-hand side) or with its retention (heterozygote effect, right-hand side). The effect of *Trp53* status is also indicated. Late loss of the second *Brca2* allele occurs in some tumors, even if it is not essential for carcinogenesis and may further fuel tumor progression. Early loss of the second allele on the other hand, if tolerated, may divert tumor evolution down a distinct trajectory, toward acinar-cell carcinomas.

a functional *Brca2* allele. Consistent with these results, we also demonstrate that three out of four human ductal pancreatic cancers arising in carriers of the $BRCA2^{999del5}$ mutation do not exhibit LOH at the mutation site. Together, these findings offer strong evidence that somatic deletion of the second *BRCA2* allele is not always necessary for carcinogenesis, revising current conceptual understanding of the tumor suppressive role of BRCA2. Interestingly and in support of our model, heterogeneous loss of the second allele was recently reported in twelve cases of human *BRCA2*-linked breast cancer (King et al., 2007), lending further weight to our suggestion. It will therefore be important to reassess the widely held view (Gudmundsson et al., 1995; Osorio et al., 2002) that the second *BRCA2* allele is consistently lost in human breast, ovarian, pancreatic, or other tumors arising in mutation carriers. However, we emphasize that our model does not preclude loss of the wild-type *BRCA2* allele in some of these cancers, but instead posits that this event may be less frequent than previously supposed because it is not essential for carcinogenesis. We cannot unequivocally exclude in the available human samples that the second *BRCA2* allele has been silenced or affected by deleterious intragenic mutations, possibilities that require further investigation using larger sample groups.

Interestingly, three pancreatic tumors from $BRCA2^{999del5}$ mutation carriers that showed evidence of LOH at the mutation site were classified as acinar-cell carcinomas. This histological type normally constitutes only 1%–2% of all pancreatic neoplasms (Hruban et al., 2007), making it unlikely that this clustering has occurred by chance. Also, an acinar-carcinoma component was exclusively observed in the $KPCB^{Tr/\Delta11}$ mouse cohort with enforced, early, biallelic *Brca2* inactivation, a phenotype not encountered in any of the 30 $KPCB^{Tr/WT}$ or $KPCB^{WT/WT}$ mice. Thus, our findings raise the possibility that LOH in *Brca2*, when it occurs early and is tolerated, can divert pancreatic carcinogenesis down a distinct evolutionary pathway.

Our results indicate that the activation of oncogenes like *Kras* may unmask the cancer-promoting effect of *Brca2* heterozygosity, which has not been previously observed in murine models in which *Brca2* alone is conditionally or constitutively inactivated (Evers and Jonkers, 2006). Whether this phenotype reflects a unique cooperative effect between oncogenic $Kras^{G12D}$ and mono-allelic *Brca2* mutations or a more broadly applicable principle for the effect of *Brca2* dosage on oncogene activation is at present unknown.

Significantly, our work suggests that the integrity of *Trp*53 shapes the cellular outcome of the second *Brca2* allele loss during carcinogenesis; thus, *Brca2* LOH in cells with intact *Trp53* may favor cell death rather than outgrowth (Jonkers et al., 2001; Ludwig et al., 1997). In the setting of inactive *Trp53*, on the other hand, biallelic *Brca2* inactivation leads to rapid tumor progression, as evidenced by the dramatically curtailed PDAC-free survival of $KPCB^{Tr/\Delta11}$ mice, suggesting that the loss of the second *Brca2* allele is tolerated and fuels tumor progression under these conditions. Indeed, our data raise the possibility that in the fraction of pancreatic tumors where the second allele is lost, this event may have occurred late in the tumorigenic process, subsequent to the inactivation of *TP53* (and/or other checkpoint genes, whose loss is similarly permissive). Support for this possibility comes from studies on samples from three human pancreatic ductal adenocarcinomas, in which *BRCA2* LOH appeared to be a late event (Goggins et al., 2000). Moreover, selection against complete *BRCA2* inactivation may persist even in established tumors as suggested by the failure to disrupt both alleles using gene targeting in a pancreatic cancer cell line (Gallmeier et al., 2007).

Taken together, our findings, and the revised model for tumor suppression by BRCA2 that they suggest, have several implications for cancer therapy. The clinical use of drugs such as PARP1 (insert 1 as before) inhibitors that selectively kill cancer cells homozygous but not heterozygous for *BRCA2* mutations (Bryant et al., 2005; Farmer et al., 2005) is based on the premise that the wild-type *BRCA2* allele is consistently deleted in tumor cells. Consequently, patient selection for these therapies currently relies on the documentation of *BRCA2* mutation carrier status using normal tissues (usually, peripheral blood mononuclear cells). However, our data raise the possibility that a proportion of PDACs arising in mutation carriers will retain a functional *BRCA2* allele, and may exhibit resistance to targeted therapies like PARP1 inhibitors. We therefore suggest that these agents should preferably be used after LOH is confirmed in tumor

samples. In the specific setting of pancreatic acinar-cell carcinomas arising in *BRCA2* mutation carriers, however, our findings suggest that biallelic *BRCA2* inactivation may be more frequent. Targeted therapies could therefore be of particular value for this histological type, a suggestion that warrants further examination. Thus, our work using a murine model that faithfully recapitulates tissue-specific familial carcinogenesis in *BRCA2* mutation carriers revises current concepts for disease pathogenesis and helps to inform the design of clinical trials using targeted agents.

EXPERIMENTAL PROCEDURES

Animal Strains, Husbandry, and Maintenance

LSL-*Kras*$^{G12D/+}$;LSL-*Trp53*$^{R270H/+}$; *Brca2*$^{F11/WT}$ animals were generated by crossing the previously described LSL-*Kras*$^{G12D/+}$;LSL-*Trp53*$^{R270H/+}$ (Olive et al., 2009) and *Brca2*$^{F11/WT}$ (Jonkers et al., 2001) strains, the latter backcrossed six times to the FVB/N background. *Pdx1*-Cre; *Brca2*$^{Tr/WT}$ double-transgenic mice were generated by crossing the previously described *Pdx1*-Cre transgenic (Hingorani et al., 2005; Olive et al., 2009) and *Brca2*$^{Tr/WT}$ (Friedman et al., 1998) strains (the latter also backcrossed six times to the FVB/N background). These strains were interbred to generate the experimental animals used in the study. Thus, all experiments were performed using littermate mice from a mixed but uniform C57BL/6;129;FVB/N genetic background. Mice were maintained in a specific pathogen-free environment under a 12 hr light/dark cycle. The animals were euthanized using a Schedule 1 method when they met predetermined severity endpoint criteria. All experiments were performed in accordance with national and institutional guidelines, and the study was approved by the ethical review committee of the University of Cambridge.

Generation of PDAC Cell Lines

Pancreatic cancer cell lines from explanted murine tumors were established using previously published methods (Schreiber et al., 2004; Olive et al., 2009). All experiments reported in this study were conducted in early passage cell lines ($\leq$P10) grown in complete medium (DMEM+10%FBS+1% Penicillin/Streptomycin).

Statistical Analyses

All statistical analyses were performed using GraphPad Prism version 5.01 for Windows (GraphPad Software, San Diego, CA). Kaplan-Meier estimates of pancreatic cancer-free survival were compared using the log-rank test. A Bonferroni-corrected p value $\leq$ 0.0167 was considered statistically significant, in order to account for the three possible individual comparisons between strains. Deaths due to causes other than pancreatic cancer were treated as censored observations. The IC_{50} values for MMC and Olaparib were grouped according to the *Brca2* status of the corresponding PDAC cell lines and compared using the Kruskal-Wallis test. Pair-wise comparisons between individual genotypes were based on Dunn's post-test. Scatter plots depict the range and median values. The nonparametric Kruskal-Wallis test was also used to compare the average number of cleaved caspase-3-positive cells per 20x field in pancreata from 6 day old neonatal mice grouped according to their genotype and Dunn's post-test was again used for pair-wise comparisons. A p value < 0.05 was considered significant in both cases.

Rad51 Foci Formation

One hundred thousand cells of the indicated genotypes were plated on coverslips (22x22 mm) in 6 well plates and allowed to grow overnight before treatment with 100 ng/ml of Mitomycin C (Sigma-Aldrich) for 24 hr. Cells were washed free of medium using PBS, fixed in 4% paraformaldehyde (PFA) for 10 min at room temperature, and then stained with a mouse monoclonal antibody to Rad51 (14B4, Santa Cruz Biotechnology) at a dilution of 1:1000 following a previously described protocol (Ayoub et al., 2009). Coverslips were imaged on a Zeiss LSM510 Meta confocal microscope, using a 40x objective. Quantification of Rad51 nuclear foci was performed as previously described (Ayoub et al., 2009). A minimum of 800 cells were analyzed in each sample to determine the average number of nuclear foci per cell. The data were exported in Excel format and plotted in Graphpad Prism v5.01.

Viability and Apoptosis Assays

Murine PDAC cell lines maintained in the logarithmic phase of growth were trypsinized, passed through a 70 μm nylon cell strainer to remove cell clumps, counted, and plated at 2500 cells/well in 96 well plates in a total volume of 100 μl of complete medium. Five wells were plated per drug concentration per cell line. Twenty-four hours later, the medium was replaced with a medium that contained increasing concentrations of Mitomycin C (Sigma-Aldrich) or Olaparib (JS Research Chemicals Trading). All cells treated with Olaparib were exposed to the same concentration of vehicle (DMSO). Cell viability was assessed following 72 hr exposure to drug, using the Cell Titer Blue Viability Assay (Promega) according to the manufacturer's instructions. Results were plotted as mean values with standard deviations (n = 5 for each different drug concentration). Curve fits were generated using nonlinear regression function (Graphpad Prism). For quantification of apoptosis, we used the Apo-ONE Homogeneous Caspase-3/7 Assay (Promega) according to the manufacturer's instructions. Apoptosis was quantified 48 hr after addition of Olaparib or vehicle and expressed as a fold increase in activity compared with vehicle-only treated cells, adjusted for cell viability that was assessed as previously described. For western blotting for cleaved caspase-3, cells were treated with 2.5 μM of Olaparib for 48 hr before harvesting.

Histology, Histochemistry, and Immunohistochemistry

Explanted tissues were fixed in 10% neutral-buffered formalin solution for 24 hr and transferred to 70% ethanol. Tissues were embedded in paraffin, cut in 5μm sections on poly-lysine coated slides, deparaffinized, rehydrated, and stained with H&E. The alcian blue and dPAS histochemical stains were performed according to established protocols (www.IHCWorld.com). Images were collected on an Olympus BX51 microscope using cellB software. For immunohistochemistry, following standard deparaffinization and rehydration, sections were unmasked in 10 mM citric acid (pH 6.0) in a microwave for 12.5–20 min depending on the antigen. Endogenous peroxidases were quenched in 3% H2O2/PBS for 15 min. Remaining steps were according to the Vectastain Elite ABC kit (rabbit) flowchart (Vector Labs, Burlingame, CA). The following primary antibodies were used: rabbit polyclonal antibody to Cytokeratin-19 (ab15463, Abcam, 1:100) and rabbit anti-cleaved caspase-3 polyclonal antibody (#9661, Cell Signaling Technology, 1:100). Primary antibody incubation was performed overnight (16 hr) at 4°C and detection was assessed using the ImmPACT DAB peroxidase substrate (Vector Labs). For fluorescent immunohistochemistry following deparaffinization, rehydration, and antigen retrieval, sections were blocked for 30 min (RT) with 10% normal goat serum (Jackson ImmunoResearch Laboratories, 005-000-001) in TBS-Tween supplemented with 0.2% Triton X-100. Primary antibody incubation was performed overnight (4°C) in TBT (1X TBS, 0.1% bovine serum albumin, 0.2% Triton X-100) using rabbit anti-γH2AX polyclonal antibody (ab2893, Abcam, 1:200) and guinea pig anti-insulin polyclonal antibody (Dako, A0564,1:100). Following secondary antibody incubation with AlexaFluor 488 goat anti-guinea pig and AlexaFluor 568 goat anti-rabbit secondary antibodies (Molecular Probes, Invitrogen), both at 1:1000 dilution in TBT for 30 min at 37°C, slides were mounted with Vectashield medium containing DAPI (Vector Laboratories, H-1200), covered with coverslips, and imaged on a Zeiss LSM510 Meta confocal microscope using a 40x objective. Images were acquired using constant zoom and imaging parameters (laser intensities and detector settings).

Laser-Capture Microdissection and Genomic PCRs

Microdissection of murine cancerous ducts was performed with the Zeiss P.A.L.M. system using 5μm tissue sections cut onto membrane-coated slides (Zeiss). DNA was extracted using the QIAamp DNA Micro Kit (QIAGEN) following the manufacturer's protocol. 1-3 ng of extracted DNA was used in PCR reactions to detect the conditional and recombined alleles. Primer pairs for individual PCR reactions are included in Supplemental Experimental Procedures. PCR conditions have been previously published (Hingorani et al., 2005; Jonkers et al., 2001; Perez-Mancera and Tuveson, 2006).

BRCA2^{999del5} LOH Analysis in Human Pancreatic Cancer Samples

Pancreatic tumor samples were obtained from patients that participated in earlier studies of familial BRCA-related cancers with permission from the Data Protection Authority (PV2006050307) and the National Bioethics

Committee (Iceland) (VSNb2006050001/03-16). Histological material available from these pancreatic tumors was evaluated and viable representative tumor tissue selected. Representative samples were subsequently dissected from 15 μm-thick sections of paraffin-embedded blocks. Genomic DNA was extracted following standard procedures for deparaffinization, rehydration, and crosslink removal using the High-Pure PCR template preparation kit (Roche) according to the manufacturer's instructions. Allele-specific quantitative PCR (qPCR) reactions to quantitatively determine the relative proportions of the wild-type and 999 del5 *BRCA2* alleles were carried out using the 7500 Realtime PCR system (Applied Biosystems). We used a TaqMan method with a single *BRCA2* specific, minor groove binding (MGB) probe (5′-end labeled with FAM, and with a nonfluorescent quencher at the 3′ end), a single *BRCA2* specific forward primer, and two allele-specific reverse primers. Therefore, the PCR for wild-type and mutant alleles was performed in separate wells. Details of the qPCR primers and TaqMan-MGB probe can be found in Supplemental Experimental Procedures. The *BRCA2* wild-type to mutant-allele ratios were quantified by measuring differences in fluorescence intensity of FAM performed in duplicate and the Ct values (number of cycles to reach intensity threshold) averaged. The wild-type to mutant allele ratios were calculated to wild-type allele frequencies by the following equation as previously described (Germer et al., 2000): frequency of allele$_1$ = $1/(2^{\Delta Ct}+1)$, where ΔCt = (Ct of allele$_1$ – Ct of allele$_2$).

Western Blotting

Logarithmically growing, spontaneously immortalized MEFs and cells from established PDAC lines were harvested by trypsinization and lysed in ice-cold RIPA lysis buffer (50 mM Tris-HCL [pH 7.4], 150 mM NaCl, 0.5% (v/v) deoxycholate, 0.1% (v/v) SDS and 1% (v/v) Igepal), supplemented with 1 mM DTT, 1mM PMSF, protease inhibitors (Amersham), and phosphatase inhibitor cocktails 1 and 2 (Sigma). Protein concentration was quantified using the BCA assay (Sigma). Total protein (100 μg) was resolved in 3%–8% Tris-Acetate precast Midi gels (Invitrogen) according to the manufacturer's protocol and transferred to PVDF membranes under semi-dry conditions using the Multiphor II electrophoresis system (Amersham). Membranes were blocked in 5% nonfat dry milk in TBS-Tween (150 mM NaCl, 5 mM Tris-HCL [pH 7.4]), and blotted with primary antibodies: rabbit polyclonal antibody against the N terminus of murine Brca2 (Sarkisian et al., 2001) (1:500), mouse monoclonal anti-β-actin (1:5000, Sigma-Aldrich), and horseradish peroxidase-conjugated anti-mouse and anti-rabbit secondary antibodies, both used at 1:10000 dilution. Signal was developed with the ECL Plus detection reagent for Brca2 and with ECL for β-actin (Amersham). Western blotting for cleaved caspase-3 was performed in the same way using a rabbit monoclonal antibody (#9664, Cell Signaling Technology) at 1:1000 dilution.

Southern Blotting

Genomic DNA from pancreatic tumors was prepared using the DNeasy kit (QIAGEN) according to the manufacturer's instructions. Genomic DNA (7.5 μg) was digested with EcoRI, and southern blot was set up with the alkaline transfer method, using the Hybond-XL membrane from Amersham. Prehybridization was carried out overnight with hybridization buffer (5× SSC, 5× Denhardt's reagent, and 0.1% SDS). DNA probe generated using the primers *Brca2* 3′ Probe Forward and *Brca2* 3′ Probe Reverse (see Supplemental Experimental Procedures) was labeled radioactively with 32PdCTP and allowed to hybridize overnight. Images were acquired using either a FUJIFILM FLA-5000 Image Reader or on X-ray film developed after 7–8 days incubation at −80°C. The ratio of the intensities of the bands corresponding to the wild-type and mutant *Brca2* allele were densitometrically quantified.

Quantitative RT-PCR

Real-time quantification of mRNA corresponding to the C terminus of murine *Brca2* using SYBR green was carried out with the Roche 480 light cycler. Normalization and target to reference ratios were calculated according to the manufacturer's instructions (Roche). RNA extraction from PDAC cell lines was carried out using the RNeasy kit (QIAGEN) according to the accompanying protocol. Total RNA (2 μg) was converted to cDNA using the M-MLV Reverse Transcriptase kit (Invitrogen). Primers *Brca2* 22 Forward and *Brca2* 24 Reverse (see Supplemental Experimental Procedures) were used to quantify the levels of cDNA corresponding to the 3′ end of murine *Brca2* in each sample. Levels of amplified *Gapdh* cDNA were used as the reference.

SUPPLEMENTAL INFORMATION

Supplemental Information includes four figures and Supplemental Experimental Procedures and can be found with this article online at doi:10.1016/j.ccr.2010.10.015.

ACKNOWLEDGMENTS

We thank the past and present members of the Venkitaraman and Tuveson laboratories for helpful comments. We thank Jos Jonkers and Anton Berns (Netherlands Cancer Institute) for the *Brca2*$^{F11/WT}$ mouse strain, and Lewis A. Chodosh (University of Pennsylvania) for the rabbit polyclonal antibody against the N terminus of murine Brca2. F.S. was supported in A.R.V.'s laboratory by studentships from the Medical Research Council (MRC) and Onassis Foundation, and subsequently by a Cancer Research UK Clinical Research Training Fellowship. L.D.C. was supported by a Cancer Research UK Molecular Pathology of Cancer studentship in A.R.V.'s laboratory. Work in A.R.V.'s laboratory is supported by the MRC. The authors declare no competing financial interests.

Received: May 27, 2010
Revised: August 25, 2010
Accepted: October 18, 2010
Published online: November 4, 2010

REFERENCES

Audeh, M.W., Carmichael, J., Penson, R.T., Friedlander, M., Powell, B., Bell-McGuinn, K.M., Scott, C., Weitzel, J.N., Oaknin, A., Loman, N., et al. (2010). Oral poly(ADP-ribose) polymerase inhibitor olaparib in patients with *BRCA1* or *BRCA2* mutations and recurrent ovarian cancer: a proof-of-concept trial. Lancet *376*, 245–251.

Ayoub, N., Rajendra, E., Su, X., Jeyasekharan, A.D., Mahen, R., and Venkitaraman, A.R. (2009). The carboxyl terminus of *Brca2* links the disassembly of Rad51 complexes to mitotic entry. Curr. Biol. *19*, 1075–1085.

Breast Cancer Linkage Consortium T. (1999). The Breast Cancer Linkage Consortium: cancer risks in *BRCA2* mutation carriers. J. Natl. Cancer Inst. *91*, 1310–1316.

Bryant, H.E., Schultz, N., Thomas, H.D., Parker, K.M., Flower, D., Lopez, E., Kyle, S., Meuth, M., Curtin, N.J., and Helleday, T. (2005). Specific killing of *BRCA2*-deficient tumours with inhibitors of poly(ADP-ribose) polymerase. Nature *434*, 913–917.

Caldas, C., and Kern, S.E. (1995). K-ras mutation and pancreatic adenocarcinoma. Int. J. Pancreatol. *18*, 1–6.

Chen, P.L., Chen, C.F., Chen, Y., Xiao, J., Sharp, Z.D., and Lee, W.H. (1998). The BRC repeats in *BRCA2* are critical for RAD51 binding and resistance to methyl methanesulfonate treatment. Proc. Natl. Acad. Sci. USA *95*, 5287–5292.

Collins, N., McManus, R., Wooster, R., Mangion, J., Seal, S., Lakhani, S.R., Ormiston, W., Daly, P.A., Ford, D., Easton, D.F., et al. (1995). Consistent loss of the wild type allele in breast cancers from a family linked to the *BRCA2* gene on chromosome 13q12-13. Oncogene *10*, 1673–1675.

Couch, F.J., Johnson, M.R., Rabe, K.G., Brune, K., de Andrade, M., Goggins, M., Rothenmund, H., Gallinger, S., Klein, A., Petersen, G.M., et al. (2007). The prevalence of *BRCA2* mutations in familial pancreatic cancer. Cancer Epidemiol. Biomarkers Prev. *16*, 342–346.

Evers, B., and Jonkers, J. (2006). Mouse models of *BRCA1* and *BRCA2* deficiency: past lessons, current understanding and future prospects. Oncogene *25*, 5885–5897.

Farmer, H., McCabe, N., Lord, C.J., Tutt, A.N., Johnson, D.A., Richardson, T.B., Santarosa, M., Dillon, K.J., Hickson, I., Knights, C., et al. (2005). Targeting the DNA repair defect in BRCA mutant cells as a therapeutic strategy. Nature *434*, 917–921.

Fong, P.C., Boss, D.S., Yap, T.A., Tutt, A., Wu, P., Mergui-Roelvink, M., Mortimer, P., Swaisland, H., Lau, A., O'Connor, M.J., et al. (2009). Inhibition of poly(ADP-ribose) polymerase in tumors from BRCA mutation carriers. N. Engl. J. Med. *361*, 123–134.

Fong, P.C., Yap, T.A., Boss, D.S., Carden, C.P., Mergui-Roelvink, M., Gourley, C., De Greve, J., Lubinski, J., Shanley, S., Messiou, C., et al. (2010). Poly(ADP)-ribose polymerase inhibition: frequent durable responses in BRCA carrier ovarian cancer correlating with platinum-free interval. J. Clin. Oncol. *28*, 2512–2519.

Friedman, L.S., Thistlethwaite, F.C., Patel, K.J., Yu, V.P., Lee, H., Venkitaraman, A.R., Abel, K.J., Carlton, M.B., Hunter, S.M., Colledge, W.H., et al. (1998). Thymic lymphomas in mice with a truncating mutation in *Brca2*. Cancer Res. *58*, 1338–1343.

Gallmeier, E., Hucl, T., Calhoun, E.S., Cunningham, S.C., Bunz, F., Brody, J.R., and Kern, S.E. (2007). Gene-specific selection against experimental fanconi anemia gene inactivation in human cancer. Cancer Biol. Ther. *6*, 654–660.

Germer, S., Holland, M.J., and Higuchi, R. (2000). High-thoroughput SNP allele-frequency determination in pooled DNA samples by kinetic PCR. Genome Res. *10*, 258–266.

Goggins, M., Schutte, M., Lu, J., Moskaluk, C.A., Weinstein, C.L., Petersen, G.M., Yeo, C.J., Jackson, C.E., Lynch, H.T., Hruban, R.H., et al. (1996). Germline BRCA2 gene mutations in patients with apparently sporadic pancreatic carcinomas. Cancer Res. *56*, 5360–5364.

Goggins, M., Hruban, R.H., and Kern, S.E. (2000). *BRCA2* is inactivated late in the development of pancreatic intraepithelial neoplasia: evidence and implications. Am. J. Pathol. *156*, 1767–1771.

Gudmundsson, J., Johannesdottir, G., Bergthorsson, J.T., Arason, A., Ingvarsson, S., Egilsson, V., and Barkardottir, R.B. (1995). Different tumor types from *BRCA2* carriers show wild-type chromosome deletions on 13q12-q13. Cancer Res. *55*, 4830–4832.

Hahn, S.A., Greenhalf, B., Ellis, I., Sina-Frey, M., Rieder, H., Korte, B., Gerdes, B., Kress, R., Ziegler, A., Raeburn, J.A., et al. (2003). *BRCA2* germline mutations in familial pancreatic carcinoma. J. Natl. Cancer Inst. *95*, 214–221.

Hezel, A.F., Kimmelman, A.C., Stanger, B.Z., Bardeesy, N., and Depinho, R.A. (2006). Genetics and biology of pancreatic ductal adenocarcinoma. Genes Dev. *20*, 1218–1249.

Hingorani, S.R., Petricoin, E.F., Maitra, A., Rajapakse, V., King, C., Jacobetz, M.A., Ross, S., Conrads, T.P., Veenstra, T.D., Hitt, B.A., et al. (2003). Preinvasive and invasive ductal pancreatic cancer and its early detection in the mouse. Cancer Cell *4*, 437–450.

Hingorani, S.R., Wang, L., Multani, A.S., Combs, C., Deramaudt, T.B., Hruban, R.H., Rustgi, A.K., Chang, S., and Tuveson, D.A. (2005). Trp53R172H and KrasG12D cooperate to promote chromosomal instability and widely metastatic pancreatic ductal adenocarcinoma in mice. Cancer Cell *7*, 469–483.

Hruban, R.H., Adsay, N.V., Albores-Saavedra, J., Compton, C., Garrett, E.S., Goodman, S.N., Kern, S.E., Klimstra, D.S., Kloppel, G., Longnecker, D.S., et al. (2001). Pancreatic intraepithelial neoplasia: a new nomenclature and classification system for pancreatic duct lesions. Am. J. Surg. Pathol. *25*, 579–586.

Hruban, R., Pitman, M., and Klimstra, D.S. (2007). Tumors of the Pancreas, *AFIP ATLAS of Tumour Pathology, Series IV* (Annapolis Junction, MD: American Registry of Pathology).

Jones, S., Hruban, R.H., Kamiyama, M., Borges, M., Zhang, X., Parsons, D.W., Lin, J.C., Palmisano, E., Brune, K., Jaffee, E.M., et al. (2009). Exomic sequencing identifies PALB2 as a pancreatic cancer susceptibility gene. Science *324*, 217.

Jonkers, J., Meuwissen, R., van der Gulden, H., Peterse, H., van der Valk, M., and Berns, A. (2001). Synergistic tumor suppressor activity of *BRCA2* and p53 in a conditional mouse model for breast cancer. Nat. Genet. *29*, 418–425.

King, T.A., Li, W., Brogi, E., Yee, C.J., Gemignani, M.L., Olvera, N., Levine, D.A., Norton, L., Robson, M.E., Offit, K., et al. (2007). Heterogenic loss of the wild-type BRCA allele in human breast tumorigenesis. Ann. Surg. Oncol. *14*, 2510–2518.

Knudson, A.G., Jr. (1971). Mutation and cancer: statistical study of retinoblastoma. Proc. Natl. Acad. Sci. USA *68*, 820–823.

Ludwig, T., Chapman, D.L., Papaioannou, V.E., and Efstratiadis, A. (1997). Targeted mutations of breast cancer susceptibility gene homologs in mice: lethal phenotypes of *Brca1*, *Brca2*, *Brca1*/*Brca2*, *Brca1*/p53, and *Brca2*/p53 nullizygous embryos. Genes Dev. *11*, 1226–1241.

Maitra, A., and Hruban, R.H. (2008). Pancreatic cancer. Annu. Rev. Pathol. *3*, 157–188.

Mikaelsdottir, E.K., Valgeirsdottir, S., Eyfjord, J.E., and Rafnar, T. (2004). The Icelandic founder mutation *BRCA2* 999del5: analysis of expression. Breast Cancer Res. *6*, R284–R290.

Olive, K.P., Tuveson, D.A., Ruhe, Z.C., Yin, B., Willis, N.A., Bronson, R.T., Crowley, D., and Jacks, T. (2004). Mutant p53 gain of function in two mouse models of Li-Fraumeni syndrome. Cell *119*, 847–860.

Olive, K.P., Jacobetz, M.A., Davidson, C.J., Gopinathan, A., McIntyre, D., Honess, D., Madhu, B., Goldgraben, M.A., Caldwell, M.E., Allard, D., et al. (2009). Inhibition of Hedgehog signaling enhances delivery of chemotherapy in a mouse model of pancreatic cancer. Science *324*, 1457–1461.

Osorio, A., de la Hoya, M., Rodriguez-Lopez, R., Martinez-Ramirez, A., Cazorla, A., Granizo, J.J., Esteller, M., Rivas, C., Caldes, T., and Benitez, J. (2002). Loss of heterozygosity analysis at the BRCA loci in tumor samples from patients with familial breast cancer. Int. J. Cancer *99*, 305–309.

Perez-Mancera, P.A., and Tuveson, D.A. (2006). Physiological analysis of oncogenic K-ras. Methods Enzymol. *407*, 676–690.

Redston, M.S., Caldas, C., Seymour, A.B., Hruban, R.H., da Costa, L., Yeo, C.J., and Kern, S.E. (1994). p53 mutations in pancreatic carcinoma and evidence of common involvement of homocopolymer tracts in DNA microdeletions. Cancer Res. *54*, 3025–3033.

Sarkisian, C.J., Master, S.R., Huber, L.J., Ha, S.I., and Chodosh, L.A. (2001). Analysis of murine *Brca2* reveals conservation of protein-protein interactions but differences in nuclear localization signals. J. Biol. Chem. *276*, 37640–37648.

Schreiber, F.S., Deramaudt, T.B., Brunner, T.B., Boretti, M.I., Gooch, K.J., Stoffers, D.A., Bernhard, E.J., and Rustgi, A.K. (2004). Successful growth and characterization of mouse pancreatic ductal cells: functional properties of the Ki-RAS(G12V) oncogene. Gastroenterology *127*, 250–260.

Thorlacius, S., Olafsdottir, G., Tryggvadottir, L., Neuhausen, S., Jonasson, J.G., Tavtigian, S.V., Tulinius, H., Ogmundsdottir, H.M., and Eyfjord, J.E. (1996). A single *BRCA2* mutation in male and female breast cancer families from Iceland with varied cancer phenotypes. Nat. Genet. *13*, 117–119.

Thorlacius, S., Sigurdsson, S., Bjarnadottir, H., Olafsdottir, G., Jonasson, J.G., Tryggvadottir, L., Tulinius, H., and Eyfjord, J.E. (1997). Study of a single *BRCA2* mutation with high carrier frequency in a small population. Am. J. Hum. Genet. *60*, 1079–1084.

Tutt, A., Robson, M., Garber, J.E., Domchek, S.M., Audeh, M.W., Weitzel, J.N., Friedlander, M., Arun, B., Loman, N., Schmutzler, R.K., et al. (2010). Oral poly (ADP-ribose) polymerase inhibitor olaparib in patients with *BRCA1* or *BRCA2* mutations and advanced breast cancer: a proof-of-concept trial. Lancet *376*, 235–244.

van der Heijden, M.S., Brody, J.R., Dezentje, D.A., Gallmeier, E., Cunningham, S.C., Swartz, M.J., DeMarzo, A.M., Offerhaus, G.J., Isacoff, W.H., Hruban, R.H., et al. (2005). In vivo therapeutic responses contingent on *Fanconi anemia*/*BRCA2* status of the tumor. Clin. Cancer Res. *11*, 7508–7515.

Venkitaraman, A.R. (2009). Linking the cellular functions of BRCA genes to cancer pathogenesis and treatment. Annu. Rev. Pathol. *4*, 461–487.

Wong, A.K., Pero, R., Ormonde, P.A., Tavtigian, S.V., and Bartel, P.L. (1997). RAD51 interacts with the evolutionarily conserved BRC motifs in the human breast cancer susceptibility gene brca2. J. Biol. Chem. *272*, 31941–31944.

Yuan, S.S., Lee, S.Y., Chen, G., Song, M., Tomlinson, G.E., and Lee, E.Y. (1999). *BRCA2* is required for ionizing radiation-induced assembly of Rad51 complex in vivo. Cancer Res. *59*, 3547–3551.